Scientific Study & Research

Chemistry & Chemical Engineering, Biotechnology, Food Industry

ISSN 1582-540X

ORIGINAL RESEARCH PAPER

ELECTROMAGNETIC FIELD APPLICATION IN FLUIDIZATION OF METALLIC PARTICLES

Gabriela MUNTIANU¹, Ileana-Denisa NISTOR^{1*}, Diana-Carmen MIRILĂ^{2,3}, Ana-Maria GEORGESCU¹, Vasilica-Alisa ARUŞ¹, Nicoleta PLATON¹, Cosmin JINESCU^{4*}

1"Vasile Alecsandri" University of Bacau, Faculty of Engineering, Department of Chemical and Food Engineering, 157 Calea Marasesti Street, 600115, Bacau, Romania
 2"Vasile Alecsandri" University of Bacau, Faculty of Engineering, Applied Engineering Sciences Research Center, 157 Calea Marasesti Street, 600115 Bacau, Romania
 3"Vasile Alecsandri" University of Bacau, Faculty of Science, Department of Biology, 157 Calea Marasesti Street, 600115, Bacau, Romania
 4Politehnica University of Bucharest, Department of Industrial Process Equipment, 313 Splaiul Independentei Street, 060042, Bucharest, Romania

*Corresponding authors: dnistor@ub.ro, cosmin.jinescu@yahoo.com

Received: November, 25, 2024 Accepted: December, 12, 2024

Abstract: This study involves obtaining homogeneous electromagnetic field near a bed of metallic particles using two coils, by varying the distance between the coils and the intensity of the electric field. Mapping and measurement of the coaxial electromagnetic field were performed in the axial and radial directions of the magnetic field lines to determine the magnetic induction and to verify the electrical resistance. These results are important for designing an installation for the fluidization of metallic particles and for predicting the behavior of a magnetically stabilized fluidized bed (MSFB). Experimental determinations were carried out to identify the specific dynamic parameters in the MSFB by measuring the pressure drop and gas velocity as functions of the particle bed height and magnetic field intensity. The application of this electromagnetic field to metallic particles is useful for creating a fixed structure to break gas bubbles, thereby intensifying the mass transfer process. Additionally, this method enhances the stability and efficiency of the fluidized bed, making it more effective for industrial applications.

Keywords: coils, magnetic induction, magnetically stabilized fluidized bed, mass transfer process

INTRODUCTION

Numerous studies of the magnetically stabilized fluidized bed (MSFB) have appeared in the last period, but Filippov and his collaborators were the first who investigated the behavior of the fluidized bed formed by iron particles under the influence of a magnetic field and the flow of a water stream [1]. Rosensweig was one of the first researchers who described the importance of the orientation and uniformity of the applied field and who present the existence of a distinct range of superficial gas velocities between the minimum fluidization velocity and the transition velocity [2]. The magnetically stabilized fluidized beds can be applied in fine [3] and microfine coal separation [4], biological [5 – 7] and biomedical applications [8], environmental applications [9, 10], hydrodynamics studies [11, 12], and mass transfer studies [13].

From a technical point of view, magnetic field fluidization is a technique that combines classical fluidization with exposure to an electromagnetic field in order to control the movement of particles, which are particles with magnetic properties (e.g. steel particles) [14]. In order to obtain a MSFB, the particles subjected to fluidization must align with the direction and the strength of the magnetic field and to stabilize the bed particles [15]. The MSFB with metallic particles exhibits many distinct flow regimes depending on gas velocity (U_g) and magnetic field intensity (H). For exact calculations of the gas velocity, the eqn. 1 is used:

$$U_g = \frac{Q}{A_c} \tag{1}$$

where Q is gas flow (L·min⁻¹), A_c is the cross-section area of the bed, $A_c = \frac{\pi \cdot D^2}{4}$ (m²), and D is the fluidization column diameter (m).

To calculate the magnetic field intensity (H), it is necessary to first calculate the magnetic induction (B) [16]. The uniform magnetic field induction is a numerical vector quantity equal to the force (F) with which the magnetic field acts on a I m long conductor (I), through which a current intensity of I A pass, when it is placed perpendicular to the magnetic field lines, as described by eqn. 2:

$$B = \frac{F}{I \cdot I} \tag{2}$$

The magnetic field is mainly characterized by the magnetic induction (B) and the magnetic intensity (H), and is expressed by eqn. 3:

$$H = \frac{B}{\mu_0} \tag{3}$$

where μ_{θ} is the magnetic permeability of vacuum, $\mu_{\theta} = 4 \cdot \pi \cdot 10^{-7} \, (\text{N} \cdot \text{A}^{-2})$.

Figure 1 shows three fluidization regimes: packed bed, magnetically stabilized fluidized bed (MSFB), and partially stabilized bed with gas bubbles [17].

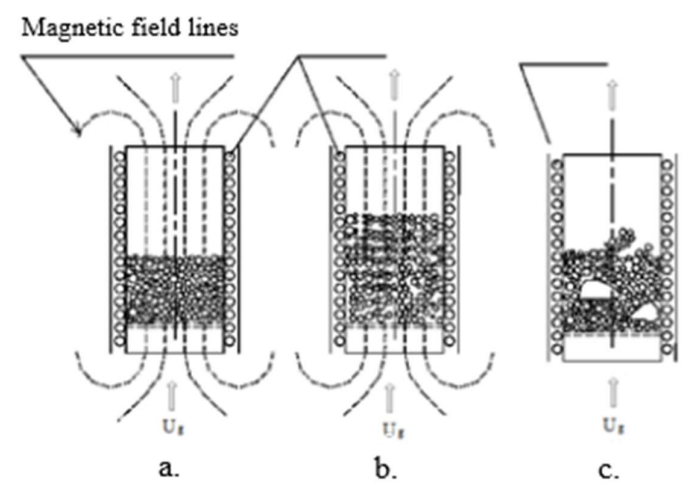


Figure 1. Structure of magnetically fluidized bed: a. packed bed; b. magnetically stabilized fluidized bed; c. partially stabilized bed [18]

Two specific gas velocities are represented in MSFB: the bed expansion velocity (U_e) and the bubbling velocity (U_b) . U_e represents the velocity at which the particle bed expansion begins for the first time with the formation of particle chains and is like the minimum fluidization velocity (U_{mf}) in classical fluidization [19]. U_b is considered the velocity at which slug formation occurs, corresponding to the pseudo-homogeneous bed structure's partial destruction because of gas bubbles [20]. The MSFB structure is maintained between those two velocities; the bed is in a stabilized state [21].

MSFB is influenced by the magnetic field intensity, the bed height, the nature and composition of the bed, the shape of solid particles, [22] humidity and temperature [23]. The orientation of the electromagnetic field lines (coaxial or transverse) in relation to the direction of the gas flow in the column is very important [24]. In the case of the coaxial field, the magnetic field lines are parallel to the direction of the gas flow and in the case of the transverse field [25], the magnetic lines are perpendicular to the column [26], as drawn in Figure 2.

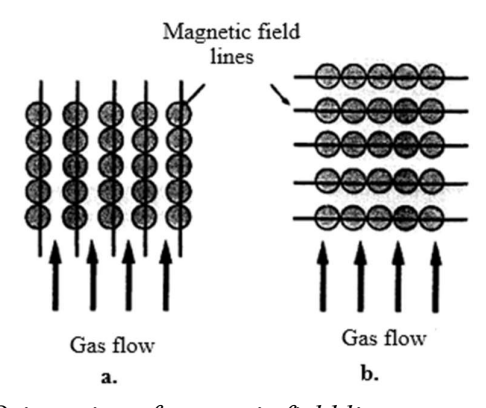


Figure 2. Orientation of magnetic field lines: a. coaxial; b. transverse

By exposing the fluidized bed to a unidirectional coaxial magnetic field that crosses the bed, the solid particles are charged with different polarities and separate from each other

[27]. This is explained by the approach of the particles to the walls of the device in the magnetic field area and the formation of small aggregates in the form of "preferential passages" that break the gas bubbles and help to unify the temperature or intensify different chemical and biochemical processes [28]. The coaxial, uniform, and steady magnetic field is the most used for creating the gas-solid magnetically stabilized fluidized bed [29].

Electromagnetic generators (electrical sources) are devices that produce and maintain electric current through a circuit, i.e., they ensure the movement of electric charge carriers through the circuit. The magnetic field can be produced by an alternating current or a direct current. The difference between them is that the interparticle attraction induced by magnetic forces is weaker for the magnetic field produced by an alternating current compared to the direct current [30].

MATERIALS AND METHODS

The fluidization tests in the presence and absence of the electromagnetic field were performed in a transparent cylindrical column where the solid particles were introduced onto the porous plate. Dry air was used as the fluidization agent in an ascending flow through the particles bed in the column with a height of 40 cm and an internal diameter of 5 cm. A pressure regulator, a gas drying column with adsorbent granules for air, and flowmeters linked in series were supplied. The fluidization agent was compressed air.

The pressure drops (ΔP) across the whole bed of particles were measured by a digital manometer that is connected to a computer, and the bed height was measured by graduated scales fitted on the column wall [31].

Before performing the particles fluidization in the coaxial electromagnetic field, it is necessary to determine the field homogeneity at all points of the fluidization column and the optimal distance between the coils [32].

In this study, electromagnets were used to generate a coaxial electromagnetic field using cylindrical coils. The coils were covered with copper wires connected in series to an electrical source with an external diameter of $16 \cdot 10^{-2}$ m and an internal diameter of $8.5 \cdot 10^{-2}$ m.

Two coils were placed symmetrically to each other on the metal stand without the fluidization column, at $5 \cdot 10^{-2}$ m and $3 \cdot 10^{-2}$ m distances between them, and connected to a continuous electric current source.

Mapping of coaxial electromagnetic field was made using a Magnet-Physik FH 51 Gauss/Teslameter equipped with a calibration capsule and a test probe. Before any measurement sets, the Teslameter was calibrated to zero in the capsule.

The particles used in these experimental studies are metallic particles with ferromagnetic properties that contain iron in a proportion of 98.5 %. This type of particle has a spherical shape that can be easily oriented in the direction of the electromagnetic field lines.

The physical properties (average particle diameter and average particles density) of the metallic particles used were determined by specific analyses [33]. The average diameter was determined experimentally by the dry sieving method, selecting the particles with a specific size range ($\overline{d}_p = 0.75 \cdot 10^{-3} m$). The particles density was determined by the volumetric method and the particles used in fluidization have an average density of a specific value $\overline{\rho}_p = 7500 \text{ kg} \cdot \text{m}^{-3}$. Measurements were taken at bed particle heights of

 $5\cdot 10^{-2}$ m and $7.5\cdot 10^{-2}$ m, varying the electromagnetic field intensity from 10987 to $47054~\text{A}\cdot\text{m}^{-1}$.

RESULTS AND DISCUSSION

Mapping and measuring of electromagnetic field

Coaxial electromagnetic field measurement with the Teslameter was carried out by checking the electrical resistance of the individual coil and measuring the magnetic induction (B) generated by the two coils at distances of $5 \cdot 10^{-2}$ m and $3 \cdot 10^{-2}$ m between them, and at different electric intensity fields between 1 A and 5 A.

In Table 1, the electric resistance (R) is checked as a function of the ratio between the voltage (U) applied to the electromagnetic circuit and the electric intensity field (I).

	Coil 1		Coil 2			
Electric voltage, U [V]	Electric intensity field, I [A]	Electric resistance, R [Ω]	Electric voltage, U [V]	Electric intensity field, I [A]	Electric resistance, R [Ω]	
15	1	15	14	1	14	
30	2	15	30.5	2	15.25 15	
45	3	15	45	3		
56	3.9	14.358	56	3.9	14.358	
Average value	_	14 839	Average value	_	14 652	

Table 1. Values obtained after calculation of electromagnetic resistance

The electromagnetic resistance of the coils is always checked for proper operation and to ensure a uniform distribution of the magnetic field lines during the particles fluidization. The average values obtained between the two coils are approximately equal, which makes the two coils work well together.

Mapping and measuring the magnetic field generated by a single coil were carried out at the six points of the coil according to Figure 3 using the Teslameter, while varying the electric intensity.

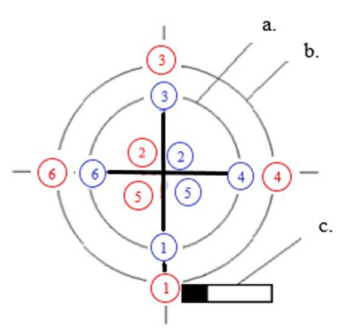


Figure 3. Measuring the magnetic field generated by a coil at various points (front view): a. upper part; b. bottom part; c. Teslameter probe

The results shown on the Teslameter display for magnetic induction (*B*) for each coil are presented in Table 2.

Table 2. Values obtained after magnetic induction measuring

Electric	Various points	Coil 1		Coil 2		
intensity field,		<i>B</i> [mT] -	<i>B</i> [mT] -	<i>B</i> [mT] -	<i>B</i> [mT] -	
I[A]		upper part	bottom part	upper part	bottom part	
	1	18.8	17.8	18.0	17.3	
	2	18.4	18.2	18.1	19.4	
1	3	19.8	20.6	20.1	20.1	
1	4	18.5	17.2	19.2	17.8	
	5	18.6	17.3	18.6	17.4	
	6	20.8	18.8	20.4	18.0	
	1	35.1	31.9	34.3	34.2	
	2	34.5	33.3	32.5	33.4	
2	3	38.2	38.3	33.0	34.8	
2	4	34.5	30.2	31.4	32.4	
	5	35.5	30.8	33.8	31.1	
	6	37.9	33.3	33.9	35.5	
	1	48.8	45.0	49.2	48.4	
	2	48.4	43.4	48.1	47.8	
3	3	53.2	49.5	50.1	50.0	
3	4	46.9	41.9	45.2	45.3	
	5	46.8	40.9	41.0	42.7	
	6	52.3	48.6	48.2	49.2	
	1	56.3	50.1	58.5	53.3	
	2	54.2	49.4	55.8	49.1	
4	3	62.3	56.1	59	59.2	
	4	53.0	47.7	51.0	49.3	
	5	54.3	47.2	50.0	51.0	
	6	60.3	51.9	53.7	53.2	

Following the results obtained when measuring the magnetic induction generated by coils 1 and 2, it is observed that the values at the six points are similar, indicating a homogeneous electromagnetic field.

Measuring of magnetic induction

For measuring the magnetic induction, the two coils were placed on a metal stand, without the fluidization column, at a distance of $L = 5 \cdot 10^{-2}$ m and $L = 3 \cdot 10^{-2}$ m between coil 1 and coil 2 (Figure 4).

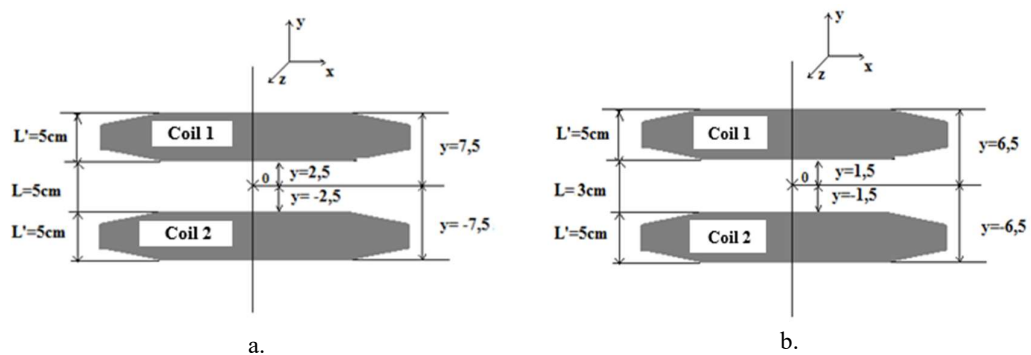


Figure 4. The placement of the two coils: $a. L = 5 \cdot 10^{-2} \text{ m}$; $b. L = 3 \cdot 10^{-2} \text{ m}$

An important characteristic of magnetic field fluidization is the possibility of maintaining the solid particles in a desired volume by placing the electromagnet at certain heights above the fluidized bed.

The magnetic induction for two coils connected to an electric source at distances of $5 \cdot 10^{-2}$ m and $3 \cdot 10^{-2}$ m between them was determined for the axial component (B_y) and radial component (B_x) as shown in Figure 5a. The position of the Teslameter probe in order to map the magnetic field of coil 1 and coil 2 is presented in Figure 5b.

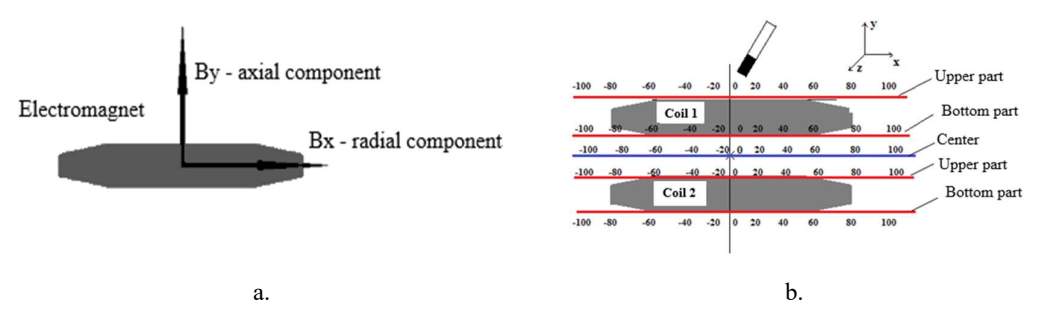


Figure 5. Measuring the magnetic induction: a. Components of the electromagnetic field; b. Mapping the magnetic field at different points

Measurements taken at 10 points from the center and at the coils' origin with the variable B_x component are shown in Figure 6.

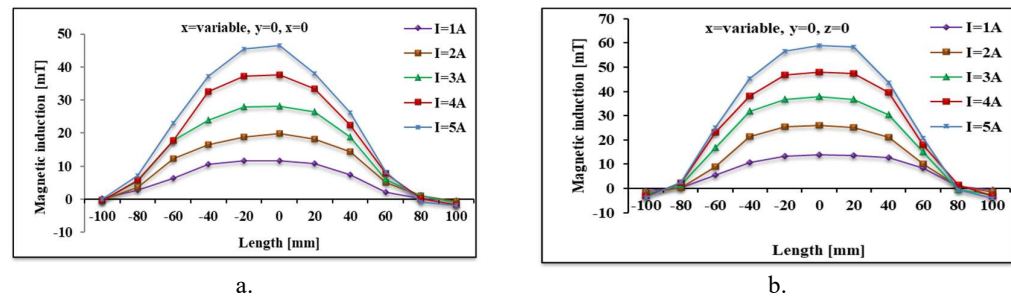


Figure 6. Magnetic induction profile according to electric intensity in coils' center and Teslameter position: $a. L = 5 \cdot 10^{-2} \text{ m}$; $b. L = 3 \cdot 10^{-2} \text{ m}$

Coaxial electromagnetic field measurement was performed at the points on the coils shown in Figure 5b.

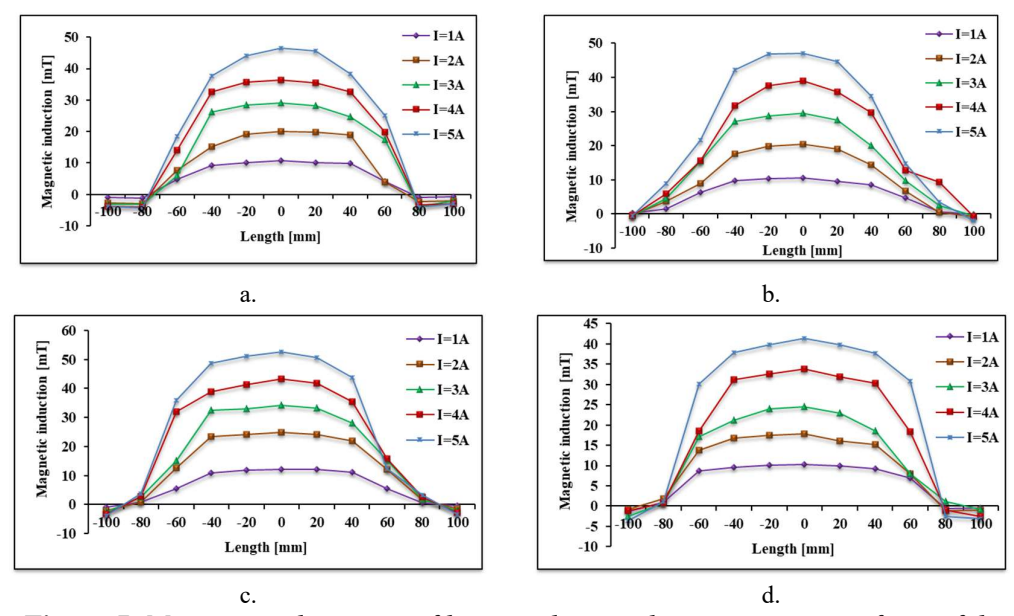


Figure 7. Magnetic induction profile according to electric intensity in front of the coils at $L = 5 \cdot 10^{-2}$ m and Teslameter position: a. x = variable, y = 7.5 cm, z = 0; b. x = variable, y = 2.5 cm, z = 0; c. x = variable, y = -2.5 cm, z = 0; d. x = variable, y = -7.5 cm, z = 0

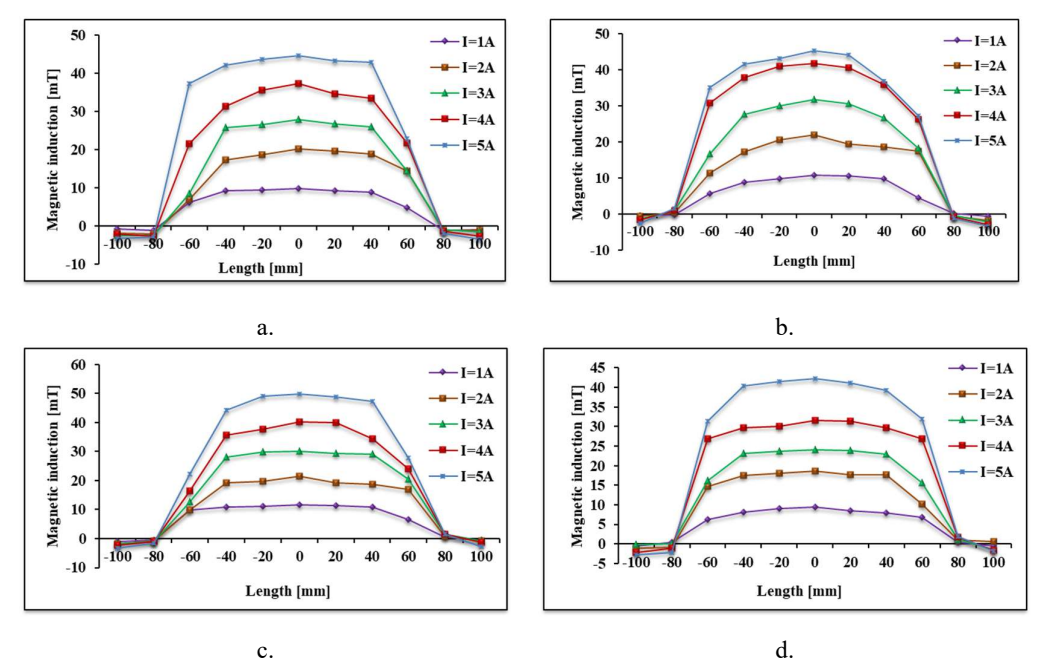


Figure 8. Magnetic induction profile according to electric intensity behind the coils at $L = 5 \cdot 10^{-2}$ m and Teslameter position: a. x = 0, y = 7.5 cm, z = variable; b. x = 0, y = 2.5 cm, z = variable; c. x = 0, y = -2.5cm, z = variable; d. x = 0, y = -7.5cm, z = variable

The experimental results regarding the measurement of the electromagnetic field for the two coils located at a distance of $3 \cdot 10^{-2}$ m between them, in front and behind of coils, can be found in the graphic representation in Figures 9 and 10.

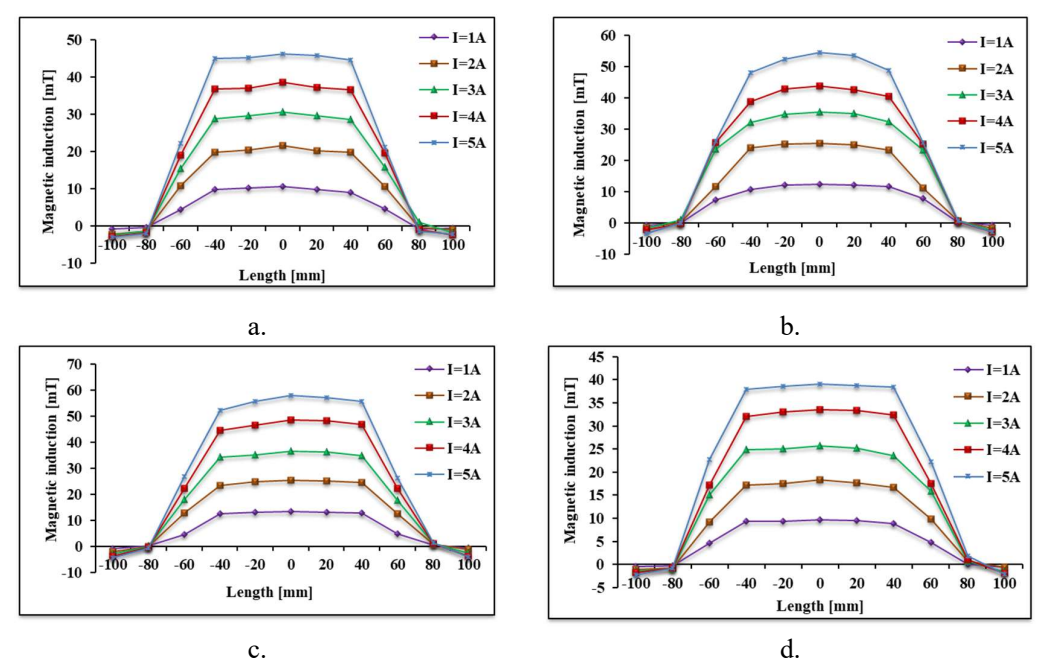
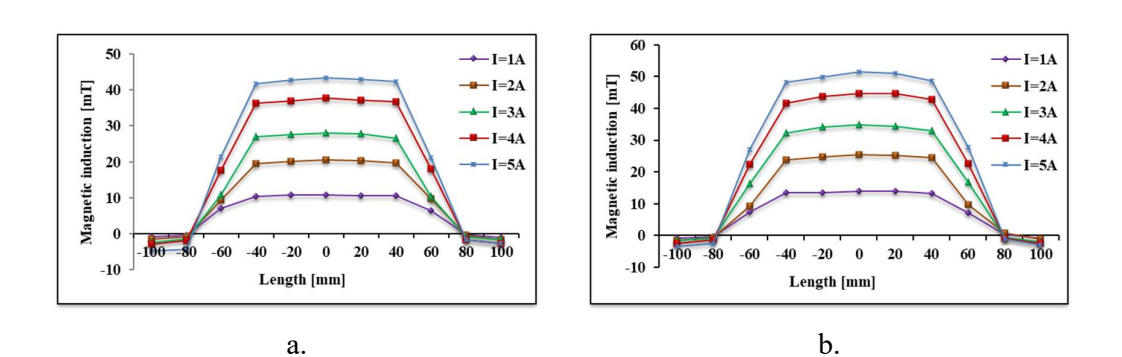
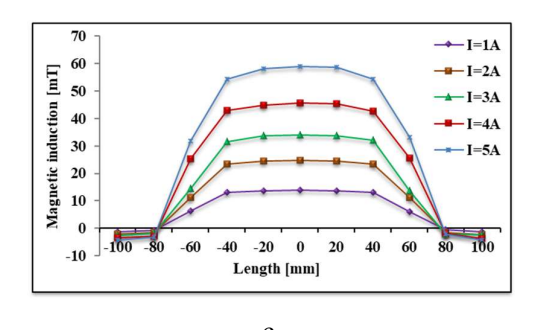


Figure 9. Magnetic induction profile according to electric intensity in front of the coils at $L = 3 \cdot 10^{-2}$ m and Teslameter position: a. x = variable, y = 6.5, z = 0; b. x = variable, y = 1.5, z = 0; c. x = variable, y = -1.5, z = 0; d. x = variable, y = -6.5, z = 0





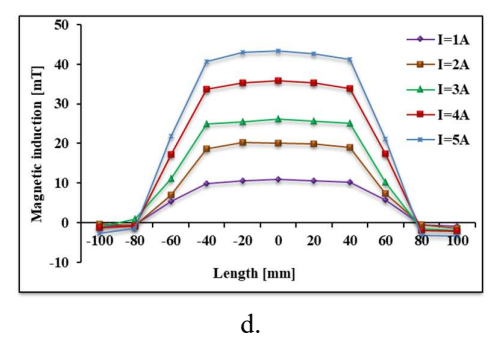


Figure 10. Magnetic induction profile according to electric intensity behind the coils at $L = 3 \cdot 10^{-2}$ m and Teslameter position: a. x = 0, y = 6.5, z = variable; b: x = 0, y = 1.5, z = variable; c: x = 0, y = -1.5, z = variable; d: x = 0, y = -6.5, z = variable

All the figures present the magnetic induction distribution in the center of the cross section for various electric intensities, and at various axial and radial measures. As expected from the graphic representations, the electromagnetic field varies linearly with the electric intensity in all the points. The fluidization tests can be performed in an electromagnetic field for bed particle heights of up to $12.5 \cdot 10^{-2}$ m.

Effect of electromagnetic field on bed pressure drop

The experiments were carried out with metallic particle masses of around 500 g, which corresponds to bed height nearly equal to $5 \cdot 10^{-2}$ m and $7.5 \cdot 10^{-2}$ m. Two coils arranged around the fluidization column at a distance of $3 \cdot 10^{-2}$ m between them produced a virtually uniform electromagnetic field. The electrical power was turned on and the fluidization agent (compressed air) was allowed to flow through the bottom inlet of the fluidization column. Gas flows of the fluidization agent, pressure drops and electromagnetic field intensity across particles bed were continuously monitored.

The particles selected in these fluidization tests have the average particles diameter of $\overline{d}_p = 0.75 \cdot 10^{-3} \, m$ and the average particles density of $\overline{\rho}_p = 7500 \, \mathrm{kg \cdot m^{-3}}$.

The establishment of the dynamic parameters in MSFB was achieved by measuring the pressure drop (ΔP) and completed with visual observations on the structure of the bed particle for each value of the gas velocity (U_g) .

In Table 3 are presented experimental values for minimum fluidization velocity (U_{mf}) and for minimum pressure drop (ΔP_{mf}) from classical fluidization (no electromagnetic field), with changes only at the bed height.

Table 3. Dynamic parameters of MSFB of metallic particles

Table 3. Dynamic parameters of MSFB of metallic particles									
No.	L_{θ} [m]	Fluidizatio	n technique	H -11	U_{mf}	$\Delta P_{\rm mf}$	U_e	ΔP_e	
Exp.			•	[A·m ⁻¹]	[m·s ⁻¹]	[Pa]	[m·s ⁻¹]	[Pa]	
1.				0	0.6784	1562.5	-	-	
2.		First fluidization	Fluidization	10987	-	-	0.7634	1875	
3.				20701	-	-	0.9328	2000	
4.				30255	-	-	1.1872	2250	
5.				38217	-	-	1.1024	2375	
6.				47054	-	-	1.1872	27000	
7.			De- fluidization	0	1.1872	1715	-	-	
8.				10987	-	-	1.272	1925	
9.				20701	-	-	1.272	1850	
10.				30255	-	-	1.272	2050	
11.				38217	-	-	1.272	2325	
12.	5.10-2			47054	-	-	1.272	2962.5	
13.	3.10		Fluidization	0	1.0176	1600	-	-	
14.				10987	-	ı	1.0176	1875	
15.				20701	-	-	1.1872	2100	
16.				30255	-	-	1.272	2750	
17.				38217	-	-	1.272	2825	
18.		Second		47054	-	-	1.3568	3100	
19.		fluidization	De- fluidization	0	0.9328	1660	-	-	
20.				10987	-	-	1.272	1925	
21.				20701	-	-	1.3568	1975	
22.				30255	-	ı	1.3568	2120	
23.				38217	-	-	1.3568	3000	
24.				47054	-		1.3568	3200	
25.				0	0.7635	2762.5	-	_	
26.			Fluidization	10987	-		1.0176	2475	
27.		First fluidization		20701	-	-	1.1875	2537.5	
28.				30255	-	-	1.272	3012.5	
29.				38217	-	-	1.272	3662.5	
30.				47054	-	-	1.272	4050	
31.			De-	0	1.0176	2700	-	-	
32.				10987	-	-	1.272	2475	
33.				20701	-	-	1.272	2287.5	
34.			fluidization	30255	-	-	1.272	2387.5	
35.	7.5·10-2		, , , , , , , , , ,	38217	_	_	1.272	2800	
36.				47054	-	-	1.272	3887.5	
37.		Second fluidization	Fluidization -	0	1.1024	2820	-	-	
38.				10987	-	-	1.1872	2700	
39.				20701	-	-	1.272	2787.5	
40.				30255	-	-	1.272	2820	
41.				38217	-	-	1.272	3125	
42.				47054	_	_	1.272	3650	
43.				0	1.0176	2700		-	
44.			De- fluidization	10987	-	-	1.1872	2575	
45.				20701	_	-	1.1872	2187.5	
46.				30255	_	-	1.1872	2312.5	
47.				38217	-	-	1.1872	2450	
48.				47054	-	-	1.1872	3375	
το.				T/UJ#		_	1.10/2	دادد	

The dynamic parameters specific to the MSFB, bed expansion velocity (U_e) and pressure drop at bed expansion (ΔP_e) are determined from the diagrams $\Delta P - U_g$ and the experimental values are also listed in Table 3.

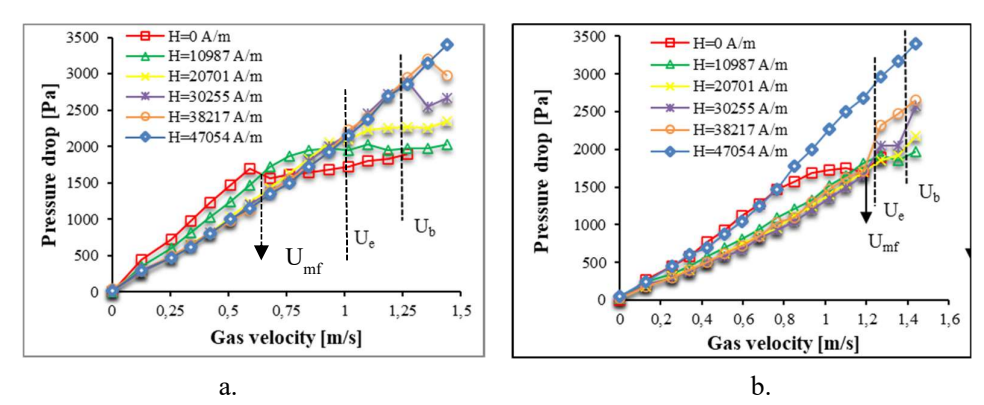


Figure 11. Influence of the electromagnetic field on the bed pressure drop at the first fluidization for metallic particles with $\overline{d}_p = 0.75 \cdot 10^{-3}$ m and $L_0 = 5 \cdot 10^{-2}$ m: a.

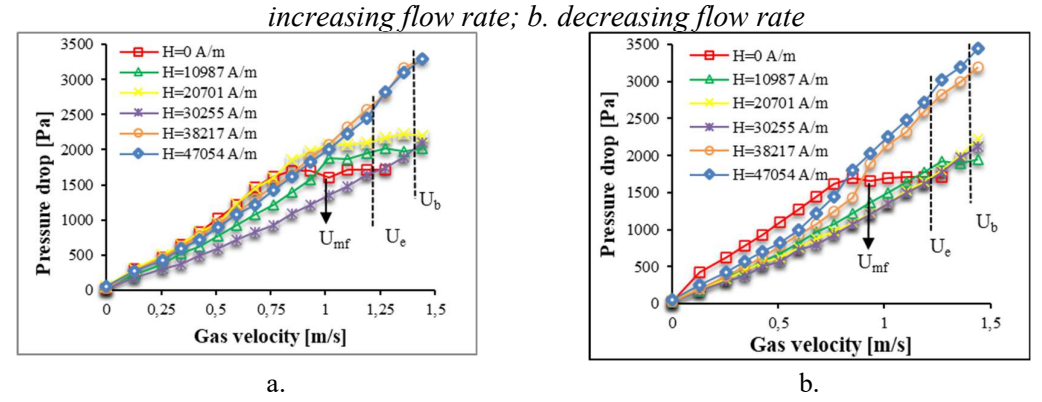


Figure 12. Influence of the electromagnetic field on the bed pressure drop at the second fluidization for metallic particles with $\overline{d}_p = 0.75 \cdot 10^{-3}$ m and $L_0 = 5 \cdot 10^{-2}$: a. increasing flow rate; b. decreasing flow rate

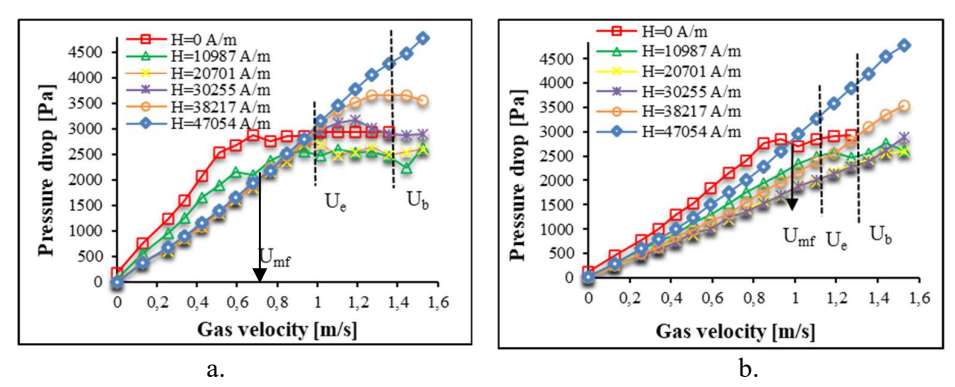


Figure 13. Influence of the electromagnetic field on the bed pressure drop at the first fluidization for metallic particles with $\overline{d}_p = 0.75 \cdot 10^{-3}$ m and $L_0 = 7.5 \cdot 10^{-2}$ m: a. increasing flow rate; b. decreasing flow rate

The particle bed structure changes in the presence of the electromagnetic field, as can be seen in the pressure drop values variation during the *first fluidization* technique (Figures 11, 13) and during the *second fluidization* technique (Figures 12, 14).

In $\Delta P - U_g$ cycles of increasing flow rate (*fluidization*) and decreasing flow rate (*de-fluidization*), the effect of coaxial electromagnetic field on the metallic particles in the column can be observed.

Increasing the U_g and H, the metallic particles arrange themselves along the coaxial electromagnetic field lines, in the direction of the gas flow, and are kept in a "quasi-fixed" position when U_e is registered.

In the electromagnetic field, the gas bubbles suppression was found above the U_b , and the metallic particles under the influence of magnetized polarization tend to rearrange themselves into a chain which limits the size of the gas bubbles.

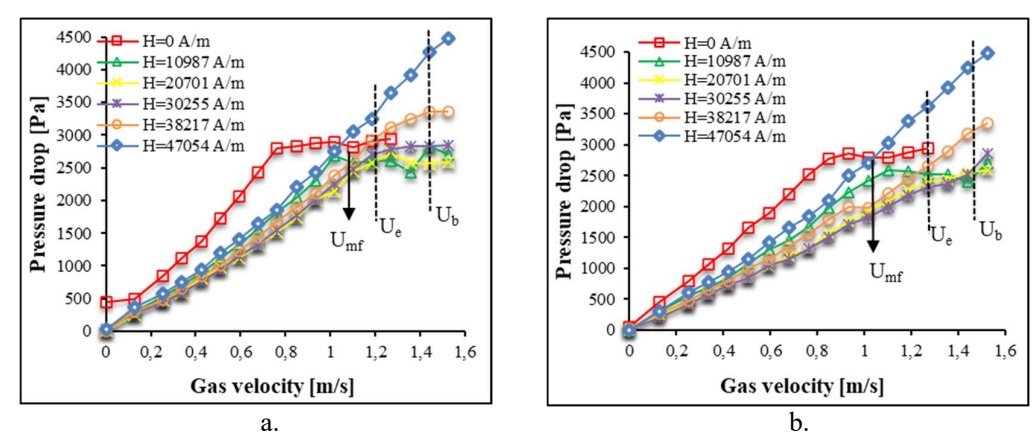


Figure 14. Influence of the electromagnetic field on the bed pressure drop at the second fluidization for metallic particles with $\overline{d}_p = 0.75 \cdot 10^{-3}$ m and $L_0 = 7.5 \cdot 10^{-2}$ m; a. increasing flow rate; b. decreasing flow rate

For the *fluidization* of these metallic particles, a coaxial electromagnetic field with intensity as low as 38217 A·m⁻¹ demonstrated the ability to induce complete bubble stabilization or elimination, and the formation of MSFB. At a high intensity of 47054 A/m, preferential passages are produced, the bed is blocked, and the gas bubbles pass through the column. During *de-fluidization*, the coaxial electromagnetic field does not stop, and the metallic particles are partially or completely locked in position. This means that the MSFB system has a structural memory as the bed subsides until becomes fixed.

CONCLUSIONS

This study of metallic particles fluidization in the electromagnetic field is important to evaluate the behavior of the MSFB. The coaxial electromagnetic field presents a spectrum formed by field lines parallel to the gas flow direction, uniformly distributed radially and axially in the fluidization column.

Metallic particles bed exhibited a classical fluidization behavior at $H = 0 \text{ A} \cdot \text{m}^{-1}$ according to literature. The fluidization agent travels up the fluidization column through the porous plate, passing through metallic particles bed depending on the gas flow rate. The metallic

particles alignment changes between the fixed bed and fluidized bed by determining the minimum fluidization velocity before large gas bubbles appear. The particles bed fluidization under the action of the coaxial electromagnetic field is a technique which reduces the gas bubbling phenomenon due to particle stabilization.

MSFB structure is a system variable depending on the electromagnetic field intensity. Magnetic forces due to particle contact generate barriers for gas bubbles. This effect is manifested as a technique of intensifying the mass transfer and the surface contact between particles and gas.

Knowledge of the dynamic parameters in obtaining the MSFB contributes to the formation of a useful database for developing future advanced plant design and exploitation.

Acknowledgements

The authors wish to express their appreciation to Mrs. Professor Gheorghita Jinescu from POLITEHNICA University of Bucharest, Faculty of Applied Chemistry and Materials Science, and to Mr. Professor Gholamreza Djelveh form Université Clermont Auvergne, France, for scientific support and technical assistance.

List of notations and symbols

```
A_c - cross-section area of the bed [m<sup>2</sup>]
```

B - magnetic induction [T]

D - fluidization column diameter [m]

 d_p - average particles diameter [m]

H - magnetic field intensity [A·m⁻¹]

I - electric intensity field [A]

L - distance between coils [m]

 L_0 - bed height [m]

l - conductor length [m]

Q - gas flow [L·min⁻¹]

R - electric resistance $[\Omega]$

U - electric voltage [V]

 U_b - bubbling velocity [m·s⁻¹]

 U_e - bed expansion velocity [m·s⁻¹]

 U_g - gas velocity [m·s⁻¹]

 U_{mf} - minimum fluidization velocity [m·s⁻¹]

 ΔP - pressure drop [Pa]

 ΔP_e - pressure drop at bed expansion [Pa]

 ΔP_{mf} - minimum pressure drop [Pa]

 μ_0 - magnetic permeability of vacuum [N·A⁻²]

 ρ_n - average particles density [kg·m⁻²]

REFERENCES

- Castelo-Grande, T., Augusto, P.A., Estevéz, A.M., Barbosa, D., Rodríguez, J.M., Álvaro, A., Torrente, C.: Magnetically Stabilized and Fluidized Beds in Science and Technology: A Review in: *Handbook of Porous Media*, 3rd edition, (Editor: Vafai, K.), CRC Press Publishers, Boca Raton, 2015, 113-156;
- 2. Hristov, J., Fachikov, L.: An overview of separation by magnetically stabilized beds: State-of-the-art and potential applications, *China Particuology*, **2007**, **5** (1-2), 11-18;
- 3. Maoming, F., Qingru, C., Yuemin, Z., Zhenfu, L., Xinxi, Z., Xiuxiang, T., Guohua, Y.: Fine coal dry classification and separation, *The European Journal of Mineral Processing and Environmental Protection*, **2003**, <u>3</u> (2), 1303-0868, 196-201;
- Tian, Y., Song, S., Xu, X., Wei, X., Yan, S., Zhan, M.: Study on Fluidization Characteristics of Magnetically Fluidized Beds for Microfine Particles, *Minerals*, 2022, 12 (1) 61;
- Al-Qodah, Z., Al-Shannag, M.: Application of Magnetically Stabilized Fluidized Beds for Cell Suspension Filtration from Aqueous Solutions, Separation Science and Technology, 2007, 42 (2), 421-438;
- Al-Qodah, Z., Al-Shannag, M., Al-Bosoul, M., Penchev, I., Al-Ahmadi, H., Al-Qodah, K.: On the performance of immobilized cell bioreactors utilizing a magnetic field, *Reviews in Chemical Engineering*, 2018, 34 (3): 385-408;
- 7. Cui, J., Li, L., Kou, L., Rong, H., Li, B., Zhang, X.: Comparing Immobilized Cellulase Activity in a Magnetic Three-Phase Fluidized Bed Reactor under Three Types of Magnetic Field, *Industrial & Engineering Chemistry Research*, **2018**, **57** (32), 10841-10850;
- 8. Odabaşi, M., Özkayar, N., Özkara, S., Ünal, S., Denizli, A.: Pathogenic antibody removal using magnetically stabilized fluidized bed, *Journal of Chromatography B*, **2005**, **826** (1-2), 50-57;
- Alonso, M., Rodríguez, N., Grasa, G., Abanades, J.C.: Modelling of a fluidized bed carbonator reactor to capture CO₂ from a combustion flue gas, *Chemical Engineering Science*, 2009, 64 (5), 883-891;
- Augusto, P.A., Castelo-Grande, T., Estevéz, A.M., Barbosa, D., Rodríguez, J. M., Álvaro, A., Sanchéz, J.: Magnetically Stabilized and Fluidized Beds: Heat and Mass Transfer, *Defect and Diffusion Forum Online*, 2008, 273-276, 46-51;
- 11. Ganzha, V.L., Saxena, S.C.: Hydrodynamic behavior of magnetically stabilized fluidized beds of magnetic particles, *Powder Technology*, **2000**, **107** (1-2), 31-35;
- 12. Zhu, Q., Li, H., Zhu, Q., Li, J., Zou, Z.: Hydrodynamic behavior of magnetized fluidized beds with admixtures of Geldart-B magnetizable and nonmagnetizable particles, *Particuology*, **2016**, **29**, 86-94:
- 13. Hausmann, R., Hoffmann, C., Franzreb, M., Höll, W.H.: Mass transfer rates in a liquid magnetically stabilized fluidized bed of magnetic ion-exchange particles, *Chemical Engineering Science*, **2000**, <u>55</u> (8), 1477-1482;
- 14. Popa, O., Ciubotariu, A.-V., Grigoras, C.C., Rosu, A.-M., Zichil, V.: Study regarding the influence of corrosive agents on the surface of metallic material like steel, *Journal of Engineering Studies and Research*, **2022**, **28** (2), 92-99;
- Hoorijani, H., Zarghami, R., Mostoufi, N.: Studying the effect of direction and strength of magnetic field on fluidization of nanoparticles by recurrence analysis, *Advanced Powder Technology*, 2022, 33 (5), 103561;
- Shaohua, G., Xiaocun, G., Jingbin, S., Baoqi, W.: Numerical Analysis and Measurement of High In-Bore Magnetic Field of Synchronous Induction Coil Launcher, *IEEE ACCESS*, 2022, 10, 3447-3458:
- 17. Zhu, Q., Gai, H., Song, H., Xiao, M., Huang, T., Hao, W.: Identification of flow regimes and determination of the boundaries for magnetized fluidized bed with Geldart-B particles, *Particuology*, **2022**, **71**, 75-89;
- 18. Fan, M., Chen, Q., Zhao, Y., Luo, Z.: Fine coal (6–1 mm) separation in magnetically stabilized fluidized beds, *International Journal of Mineral Processing*, **2001**, <u>63</u> (4), 225-232;
- Ganzha, V.L., Saxena, S.C.: A model for the calculation of minimum bubbling velocity of magnetically stabilized beds of pure and admixture particles, *Powder Technology*, 1999, 103 (2), 194-197;

- 20. Thivel, P.-X., Gonthier, Y., Boldo, P., Bernis, A.: Magnetically stabilized fluidization of a mixture of magnetic and non-magnetic particles in a transverse magnetic field, *Powder Technology*, **2004**, **139** (3), 252-257;
- 21. Rhodes, M.J., Wang, X.S., Forsyth, A.J., Gan, K.S., Phadtajaphan, S.: Use of a magnetic fluidized bed in studying Geldart Group B to A transition, *Chemical Engineering Science*, **2001**, <u>56</u> (18), 5429-5436;
- 22. Mosnegutu, E.-F., Nedeff, V., Chitimus, A.-D., Jasiński, M., Barsan, N.: Solid particle characterization. some aspect related to the shape evaluation by using software correlations, *Journal of Engineering Studies and Research*, **2021**, **27** (1), 64-74;
- Zhu Q., Li H., Huang Q.: Magnetized fluidized bed with binary admixture of magnetizable and nonmagnetizable particles, Reviews in Chemical Engineering, 2019, 35 (8), 1-34;
- 24. Ursu, A.V., Djelveh, G., Gros, F., Jinescu, G.: Hydrodynamique des mélanges ségregatifs en fluidisation sous champ magnétique transverse et coaxial in *Récents Progrès en Génie des Procédés*, no. 101, Ed. SFGP, Paris, France, **2011**;
- 25. Wanga, S., Shena, Y., Maa, Y., Gaob, J., Lanb, X., Donga, Q., Cheng, Q.: Study of hydrodynamic characteristics of particles in liquid–solidfluidized bed with uniform transverse magnetic field, *Powder Technology*, **2013**, **245**, 314-323;
- Gros, F., Baup, S., Aurousseau, M.: Hydrodynamic study of a liquid/solid fluidized bed under transverse electromagnetic field, *Powder Technology*, 2008, 183 (2), 152-160;
- 27. Hristov, J.: Magnetic field assisted fluidization a unified approach Part 1. Fundamentals and relevant hydrodynamics of gas-fluidized beds (batch solids mode), *Reviews in Chemical Engineering*, **2002**, **18** (4-5), 295-512;
- 28. Hristov, J.: Magnetic field assisted fluidization A unified approach: A series of review papers, *Reviews in Chemical Engineering*, **2002**, **18** (4-5), I-IV;
- Zhang, Q., Liu, W., Cao, Y., Gai, H., Zhu, Q.: Diverse gas-solid magnetized fluidized beds with different magnetic fields, *Powder Technology*, 2024, 433;
- Zhang, W.: A Review of Techniques for the Process Intensification of Fluidized Bed Reactors, Chinese Journal of Chemical Engineering, 2009, 17 (4), 688-702;
- 31. Muntianu, G., Ursu A.-V., Djelveh G., Isopencu G., Mares A.-M., Nistor I.D., Jinescu C.V.: Dynamic parameters for mixtures of pillared clay-magnetic particles in fluidized bed in coaxial magnetic field, *Revista de Chimie*, **2014**, **65** (9), 1077-1085;
- Ursu, A.V., Nistor, I.D., Gros, F., Arus, A.V., Isopencu, G., Mares, A.V.: Hydrodynamic aspects
 of fluidized bed stabilized in magnetic field, *U.P.B. Scientific Bulletin, Series B*, 2010, 72 (3), 8598.
- 33. Muntianu, G., Platon, N., Arus, V.A., Rosu, A.M., Nistor, D.I., Jinescu, G.: Hydrodinamic study of clay particles in fluidized bed, *Journal of Engineering Studies and Research*, **2013**, <u>19</u> (2), 70-74.